AIP | Applied Physics Letters

# Organic-free suspension of large-area graphene

E. Ledwosinska, P. Gaskell, A. Guermoune, M. Siaj, and T. Szkopek

Citation: Appl. Phys. Lett. **101**, 033104 (2012); doi: 10.1063/1.4737415
View online: http://dx.doi.org/10.1063/1.4737415
View Table of Contents: http://apl.aip.org/resource/1/APPLAB/v101/i3
Published by the AIP Publishing LLC.

# Organic-free suspension of large-area graphene

E. Ledwosinska,[1,2] P. Gaskell,[1,2] A. Guermoune,[3,4] M. Siaj,[3,4] and T. Szkopek[1,2]
[1]*Regroupement Québécois sur les Matériaux de Pointe, Montréal, Québec H3C 3J7, Canada*
[2]*Department of Electrical and Computer Engineering, McGill University, Montréal, Québec H3A 0E9, Canada*
[3]*Centre Québecois sur les Matériaux Fonctionnels, Québec, Québec G1V 0A6, Canada*
[4]*Département de Chimie, Université du Québec à Montréal, Montréal, Québec H3C 3P8, Canada*

(Received 14 May 2012; accepted 1 July 2012; published online 17 July 2012)

We report an entirely organic-free method to suspend monolayer graphene grown by chemical vapour deposition over 10–20 $\mu$m apertures in a Cu substrate. Auger electron spectroscopy, Raman spectroscopy, scanning electron microscope, and transmission electron microscope measurements confirm high quality graphene with no measurable contamination beyond that resulting from air exposure. This method can be used to prepare graphene for fundamental studies and applications where the utmost cleanliness and structural integrity are required. © *2012 American Institute of Physics*. [http://dx.doi.org/10.1063/1.4737415]

The criterion of greatest importance in fabricating samples for probing graphenes intrinsic properties is cleanliness. Owing to graphene's monolayer thickness, even a single molecular layer of foreign material on a graphene membrane can lead to contaminant species outnumbering the constituent carbon atoms of the graphene itself. Research on suspended graphene has attracted attention for a variety of reasons, owing to graphene's unique electrical,[1] mechanical,[2,3] thermal,[4] and optical[5] properties. Surface contamination resulting from the various transfer methods in common use has long been a critical problem for transmission electron microscopy (TEM),[6] Raman spectroscopy,[7] scanning tunnelling microscopy (STM),[8] mechanical studies,[9] and gas permeability studies[10] of graphene. Various methods have been reported for large-scale transfer and/or suspension of graphene, with all but one method including a critical step where graphene is coated with a polymer handle, typically polymethyl methacrylate (PMMA) or polydimethyl siloxane (PDMS),[11–16] to ensure structural rigidity for subsequent removal of the sacrificial growth substrate. While a method has been developed to transfer graphene without a handle onto a flat and continuous polymer substrate,[17] handle-free suspension of clean graphene over an aperture has proved elusive.

Efforts to remove the polymer residue following transfer have included various solvent treatments as well as thermal annealing in an effort to decompose the PMMA or other organic residue. Exhaustive solvent treatments leave polymer residue.[15,18] Thermal annealing of the residue not only results in thermal stress that causes breakage of graphene without ever completely removing the polymer from all areas but also changes graphene's electronic properties by rehybridizing carbon ortibals from $sp^2$ to $sp^3$ and modulating graphene's band structure.[7] To date, the only polymer-free method of suspension has been developed by Regan *et al.*,[19] with 1.2 $\mu$m diameter graphene membranes suspended on TEM grids using the surface tension of isopropyl alcohol to effect transfer between handles.

We report here an entirely organic-free method to suspend graphene over 10–20 $\mu$m apertures formed in a Cu substrate. There is no step of the process where the graphene is in physical contact with any chemical apart from the inorganic etchant used to etch apertures in the Cu growth substrate and water. To date, experimentalists interested in probing graphene's intrinsic properties faithfully rely on exfoliated graphene[9,20,21] to ensure clean samples despite modern advances in large-scale, monolayer chemical vapour deposition (CVD) growth of graphene. Moreover, the study of the intrinsic properties of CVD-grown graphene has been inhibited by interaction with the substrate and/or contamination arising from the transfer processes involving organics. Our organic-free method enables large-scale synthesis of clean, suspended graphene of high quality suitable for experiments that demand graphene free of contamination.

Our technique for suspending CVD-graphene may find use in the manufacture of TEM grids. Graphene has long been eyed as the ideal candidate for a TEM grid support due to its low TEM background signal,[22–24] its high electrical conductivity that minimizes charging effects from the electron beam,[22] and its superior strength[2] allowing the support of large molecules.[25] Unlike previous efforts to employ CVD-grown graphene as a TEM grid support,[13,14] our method ensures a substrate free of residue that may have a larger electron scattering cross-section than graphene itself. Other applications of our suspended membranes include pressure sensors, capacitors, and other NEMS (nanoelectromechanical system) devices.

Large-area graphene was grown by CVD on 25 $\mu$m-thick Cu foils in a split-tube furnace with $H_2$ and $CH_4$ precursors at 850 °C, with the growth procedure detailed elsewhere.[26] The device fabrication process is outlined in Fig. 1. The graphene-coated Cu foils were floated in an etchant of 0.1 M $(NH_4)_2S_2O_8$ and monitored over the course of a few hours (varying from sample to sample) to observe the first formation of etch pits (Fig. 1(a)). After the etch, the sample is placed in a water bath for rinsing and allowed to dry in air. A powerful tool in the study of plastic deformation of metals is observation of the selective attack of etchants to reveal dislocation sites in metal crystals by surface pitting.[27] Because defects in copper's fcc crystal structure are more

 

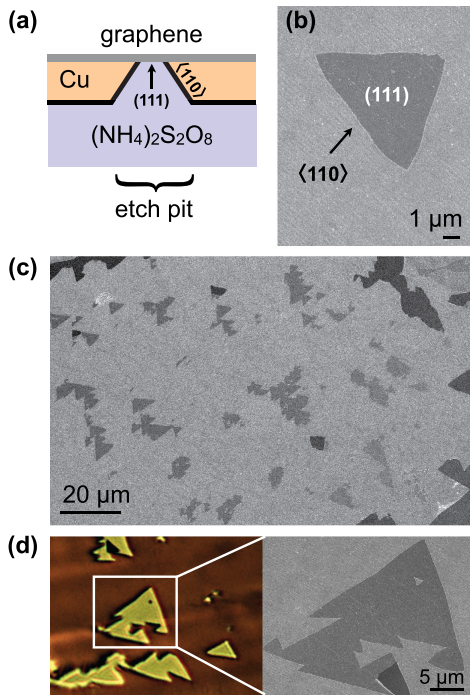


FIG. 1. (a) The fabrication process harnesses the selective attack of the etchant to defects, suspending graphene membranes over etch pits. (b) Graphene suspended over a triangular etch pit in the Cu surface, with the ⟨110⟩ edges forming the outline of the (111) surface. (c) Typical etched region of Cu depicting yield of suspended (grey) to non-suspended (black) openings. (d) Optical (left) and SEM (right) image of a Cu flake suspended on a graphene membrane, illustrating graphene's suitability for an extremely strong TEM grid support.

prone to chemical attack, etch pits most likely form along slip dislocations through to the graphene surface before the Cu foil loses significant overall thickness. Thus, graphene membranes become suspended over these apertures, with the remaining Cu serving as a supporting substrate. Etch pits are either triangular or irregular in shape, and no preference for graphene suspension over either shape of etch pit has been observed. The triangular etch pits have edges parallel to the ⟨110⟩ directions, with graphene suspended over the (111) face. The other (111) planes intersect along ⟨110⟩ directions, so that slip planes are parallel to the edges of the triangular pits as illustrated in Fig. 1(b). However, if the crystallographic orientation of the Cu surface is tilted by a few degrees from the (111) plane, the pits become irregular in shape, as seen in Fig. 1(c). As etching time is increased, the pits widen until they coalesce with neighbouring pits, and new pits form with dimensions suitable for graphene suspension. Preferential etching also occurs along grain boundaries. The largest membranes that we observed had side lengths of $\approx 20\,\mu$m, and Fig. 1(c) provides an indication of typical yield of suspended (grey) to non-suspended (black) openings.

The relatively high yield of the simple process suggests graphene's mechanical strength plays an important role in the process. Fig. 1(d) shows an optical transmission (left) and SEM image (right) of a region with a small Cu crystallite suspended on a graphene membrane. The suspended Cu mass is approximately 5 pg, which, using the areal mass density of graphene[10] $= 7.4 \times 10^{-8}$ g/cm$^2$, is a Cu/C mass ratio of 35:1. Other such suspended regions revealed graphene supporting Cu flakes up to 3000 times the membrane weight, indicating CVD graphene's supreme strength and potential for use as a TEM grid support.

Fig. 2(a) shows the Raman spectrum of the suspended membrane in (b) (optical) and (c) (SEM) measured with a diffraction limited spot at the marked location. A pump wavelength of 633 nm and a pump power of 10 mW were used. The spectrum confirms monolayer graphene and the integrated intensity ratio $I_D/I_G = 0.05$, indicating high structural quality of our suspended graphene. The defect density was estimated[28] from $I_D/I_G$ to be $5 \times 10^{10}$ cm$^{-2}$. We attribute the low disorder to the quality of the growth and to the gentle nature of the suspension process, where the graphene never leaves its original substrate. The G peak is located at 1584 cm$^{-1}$, as is expected for clean graphene where the Fermi level lies at the charge neutrality point.[29] It has previously been found[7,15] that residual PMMA on suspended graphene introduces a low frequency (1100–1600 cm$^{-1}$) broad background signal, indicative of amorphous carbon. Since the graphene membranes fabricated with our method have never contacted any large hydrocarbon molecules, the Raman spectra show no such background.

A Philips CM200 TEM was used to verify the structural integrity and cleanliness of the graphene membranes. In Fig. 3(a), monolayer graphene is seen under bright-field TEM (200 kV) as a homogeneous region, with the edge of the ruptured membrane scrolling within the field of view for contrast purposes. Fig. 3(b) was taken in the region of a wrinkle, where parallel edges indicate graphene scrolling. Electron diffraction patterns were measured on regions free of wrinkles (Fig. 3(a), inset), producing the expected hexagonal diffraction pattern for crystalline graphene. The diffraction patterns do not exhibit diffuse inner circular halos, which would indicate presence of amorphous material.

Auger electron spectroscopy (AES) was performed at 5 kV with a $3 \times 3\,\mu$m$^2$ spot size on multiple graphene membranes to verify the absence of contamination. AES is a standard surface analysis technique, allowing one to probe the elemental distribution of the first few atomic layers of a sample with high spatial resolution and precise chemical sensitivity.[30] In Fig. 4(a), we see an Auger element map, where lighter regions indicate higher fractional presence of Cu.

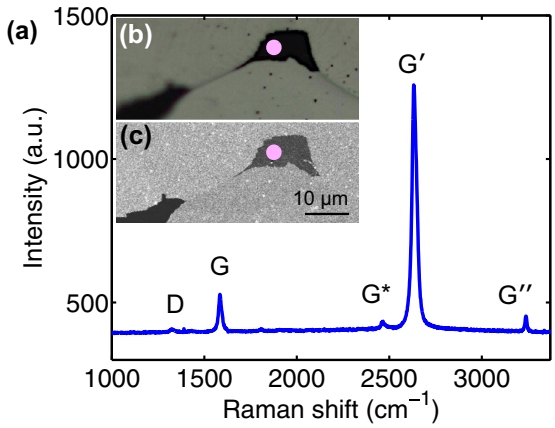


FIG. 2. (a) Raman spectrum of suspended graphene membrane exhibiting $I_D/I_G = 0.05$, indicating graphene of high structural integrity. (b) Optical and (c) SEM image of the measuring location on the suspended membrane. The etch pit formed along a Cu grain boundary.

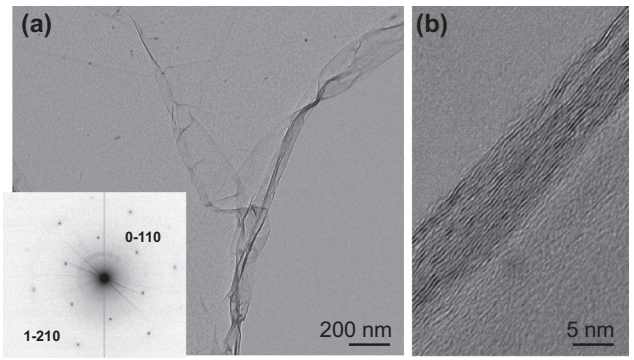


FIG. 3. (a) TEM image of ruptured membrane scrolling. Inset: electron diffraction pattern from a monolayer region, with Miller-Bravais indices (*hkil*) labeled as (0-110) (2.5 Å lattice constant) for the innermost hexagon and (1-210) (1.42 Å interatomic spacing) for the outer. (b) A wrinkled region revealing multiple lines due to numerous graphene layers.

A thicker graphene layer is evidenced by a dark line on the Cu surface. Fig. 4(b) shows the same region but probed for C KLL electrons, with the suspended region showing the highest signal strength. Again, the thicker layer of graphene at the boundary is evident now as a bright line on the Cu surface. Previous work[31] suggests that variations in graphene thickness occur at graphene grain boundaries.

The differential (Fig. 4(c)) and direct (Fig. 4(d)) AES spectra from 200–1000 eV reveal C KLL and O KLL (511 eV) electron transitions. The oxygen peak is due to covalently bonded oxygen on the graphene surface as a result of exposure to air. A high-resolution scan of the C KLL transition shows the peak at 269 eV in the AES spectrum (Fig. 4(e) and 4(f)), providing corroborating evidence of monolayer graphene on account of the non-existent kink expected at 240 eV for multiple graphene layers, and the peak position matching that found earlier for monolayer graphene[32] A sweep out to 2000 eV confirmed the absence of further peaks, indicating contamination of no more than 1% from foreign species introduced by the etchant or any other source.

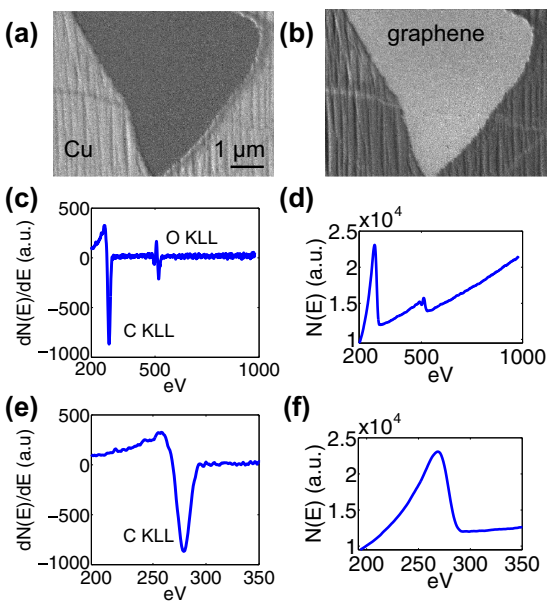


FIG. 4. (a) Auger element map of Cu showing large fractional presence of Cu (brighter areas) as well as a multilayer graphene stripe. (b) C KLL electron map of the same region. (c) Differential and direct (d) AES survey spectrum showing the presence of carbon and oxygen on a suspended graphene membrane. (e) Differential and direct (f) spectrum of the C KLL electron peak, confirming monolayer graphene.

In conclusion, we have developed an entirely organic-free method to suspend CVD-grown graphene membranes on their original growth substrate. AES, TEM, SEM, and Raman spectroscopy confirm high-quality, uncontaminated graphene, unlike other suspension methods involving polymer handles. Such high quality graphene membranes are not only desired but absolutely necessary for fundamental studies of graphene's mechanical, optical, thermal, and chemical properties where only the cleanest samples suffice.

This work was made possible by support from the Natural Science and Engineering Research Council, Le Fonds de Recherche du Québec—Nature et Technologies, the Canada Research Chairs program and the Canadian Institute for Advanced Research. We thank Josianne Lefebvre and David Liu for assistance with Auger spectroscopy and transmission electron microscopy, and Marta Cerruti for access to her Raman spectrometer.

[1]K. Bolotin, K. Sikes, Z. Jiang, M. Klima, G. Fudenberg, J. Hone, P. Kim, and H. Stormer, Solid State Commun. **146**, 351 (2008).
[2]I. Frank, D. Tannenbaum, A. van der Zande, and P. McEuen, J. Vac. Sci. Technol. B **25**, 2558 (2007).
[3]C. Lee, X. Wei, J. Kysar, and J. Hone, Science **321**, 385 (2008).
[4]A. Balandin, S. Ghosh, W. Bao, I. Calizo, D. Teweldebrhan, F. Miao, and C. Lau, Nano Lett. **8**, 902 (2008).
[5]K. Mak, M. Sfeir, Y. Wu, C. Lui, J. Misewich, and T. Heinz, Phys. Rev. Lett. **101**, 196405 (2008).
[6]K. Kim, Z. Lee, W. Regan, C. Kisielowski, M. Crommie, and A. Zettl, ACS Nano **5**, 2142 (2011).
[7]Y. Lin, C. Lu, C. Yeh, C. Jin, K. Suenaga, and P. Chiu, Nano Lett. **12**, 414 (2011).
[8]R. Decker, Y. Wang, V. Brar, W. Regan, H. Tsai, Q. Wu, W. Gannett, A. Zettl, and M. Crommie, Nano Lett. **11**, 4631 (2011).
[9]C. Chen, S. Rosenblatt, K. Bolotin, W. Kalb, P. Kim, I. Kymissis, H. Stormer, T. Heinz, and J. Hone, Nat. Nanotechnol. **4**, 861 (2009).
[10]J. Bunch, S. Verbridge, J. Alden, A. van der Zande, J. Parpia, H. Craighead, and P. McEuen, Nano Lett. **8**, 2458 (2008).
[11]X. Li, W. Cai, J. An, S. Kim, J. Nah, D. Yang, R. Piner, A. Velamakanni, I. Jung, E. Tutuc, S. Banerjee, L. Colombo, and R. Ruoff, Science **324**, 1312 (2009).
[12]S. Bae, H. Kim, Y. Lee, X. Xu, J. Park, Y. Zheng, J. Balakrishnan, T. Lei, H. Kim, Y. Song, Y. Kim, K. Kim, B. Ozyilmaz, J. Ahn, B. Hong, and S. Iijima, Nat. Nanotechnol. **5**, 574 (2010).
[13]S. Kumar, E. Rezvani, V. Nicolosi, and G. Duesberg, Nanotechnology **23**, 145302 (2012).
[14]B. Aleman, W. Regan, S. Aloni, V. Altoe, N. Alem, C. Girit, B. Geng, L. Maserati, M. Crommie, F. Wang, and A. Zettl, ACS Nano **4**, 4762 (2010).
[15]Y. Lin, C. Jin, J. Lee, S. Jen, K. Suenaga, and P. Chiu, ACS Nano **5**, 2362 (2011).
[16]J. Suk, A. Kitt, C. Magnuson, Y. Hao, S. Ahmed, J. An, A. Swan, B. Goldberg, and R. Ruoff, ACS Nano **5**, 6916 (2011).
[17]E. Lock, M. Baraket, M. Laskoski, S. Mulvaney, W. Lee, P. Sheehan, D. Hines, J. Robinson, J. Tosado, M. Fuhrer, S. Hernandez, and S. Walton, Nano Lett. **12**, 102 (2012).
[18]V. Geringer, D. Subramaniam, A. Michel, B. Szafranek, D. Schall, A. Georgi, T. Mashoff, D. Neumaier, M. Liebmann, and M. Morgenstern, Appl. Phys. Lett. **96**, 082114 (2010).
[19]W. Regan, N. Alem, B. Aleman, B. Geng, C. Girit, L. Maserati, F. Wang, M. Crommie, and A. Zettl, Appl. Phys. Lett. **96**, 113102 (2010).
[20]S. Koenig, N. Boddeti, M. Dunn, and J. Bunch, Nat. Nanotechnol. **6**, 543 (2011).
[21]Z. Ni, T. Yu, Z. Luo, Y. Wang, L. Liu, C. Wong, J. Miao, W. Huang, and Z. Shen, ACS Nano **3**, 569 (2009).
[22]J. Meyer, C. Girit, M. Crommie, and A. Zettl, Nature (London) **454**, 319 (2008).

[23]N. Wilson, P. Pandey, R. Beanland, R. Young, I. Kinlock, L. Gong, Z. Liu, K. Suenaga, J. Rourke, S. York, and J. Sloan, ACS Nano **3**, 2547–2556 (2009).
[24]G. Odahara, T. Ishikawa, S. Otani, and C. Oshima, e-J. Surf. Sci. Nanotechnol. **7**, 837 (2009).
[25]J. Sloan, Z. Liu, K. Suenaga, N. Wilson, P. Pandey, L. Perkins, J. Rourke, and I. Shannon, Nano Lett. **10**, 4600 (2010).
[26]A. Guermoune, T. Chari, F. Popescu, S. Sabri, J. Guillemette, H. Skulason, T. Szkopek, and M. Siaj, Carbon **49**, 4204 (2011).
[27]J. Livingston, J. App. Phys. **31**, 1071 (1960).
[28]M. Lucchese, F. Stavale, E. Ferreira, C. Vilani, M. Moutinho, R. Capaz, C. Achete, and A. Jorio, Carbon **48**, 1592 (2010).
[29]J. Yan, Y. Zhang, P. Kim, and A. Pinczuk, Phys. Rev. Lett. **98**, 166802 (2007).
[30]Practical surface analysis. *Auger and X-ray photoelectron spectroscopy*, 2nd ed., edited by D. Briggs and M. Seah (Wiley, New York, 1984), Vol. 1.
[31]Z. Luo, Y. Lu, D. Singer, M. Berck, L. Somers, B. Goldsmith, and A. Johnson, Chem. Mater. **23**, 1441 (2011).
[32]M. Xu, D. Fujita, J. Gao, and N. Hanagat, ACS Nano **4**, 2937 (2010).